Title: HuR-dependent SOD2 protein synthesis is an early adaptation to anchorage independence

Authors: Yeon Soo Kim[1], Jaclyn E. Welles[2], Priscilla W. Tang[1], Zaineb Javed[1], Amal T. Elhaw[1], Karthikeyan Mythreye[3], Scot R. Kimball[2], Nadine Hempel[1,4,α, β]

[1] Department of Pharmacology, College of Medicine, Pennsylvania State University, Hershey, PA, USA

[2] Department of Cellular and Molecular Physiology, College of Medicine, Pennsylvania State University, Hershey, PA, USA

[3] Department of Pathology, University of Alabama at Birmingham, Birmingham, AL, USA

[4] Department of Medicine, Division of Hematology/Oncology, UPMC Hillman Cancer Center, University of Pittsburgh, PA, USA

[α]Corresponding Author:
Nadine Hempel, Ph.D.
Department of Pharmacology
Penn State University College of Medicine
MC R130, 500 University Drive
Hershey PA 17033-0850

[β]Present Address:
University of Pittsburgh School of Medicine, Division of Hematology/Oncology
UPMC Hillman Cancer Center
Magee-Womens Research Institute, A410
204 Craft Ave, Pittsburgh, PA 15213
Ph: 412-641-7736
nah158@pitt.edu

Abstract

During metastasis, cancer cells must adapt to survive a loss of anchorage and evade anoikis. An important pro-survival adaptation is the ability of metastatic tumor cells to increase their antioxidant capacity and restore cellular redox balance. Although much is known about the transcriptional regulation of antioxidant enzymes in response to stress, how cells rapidly adapt to alter antioxidant enzyme levels is less well understood. Using ovarian cancer cells as a model, we demonstrate that an increase in protein expression of the mitochondrial superoxide dismutase SOD2 is a very early event initiated in response to cellular detachment. SOD2 protein synthesis is rapidly induced within 0.5-2 hours of matrix detachment, and polyribosome profiling demonstrates an increase in the number of ribosomes bound to *SOD2* mRNA, indicating an increase in *SOD2* translation in response to anchorage-independence. Mechanistically, we find that anchorage-independence specifically induces cytosolic accumulation of the RNA binding protein HuR/ELAVL1 and leads to increased HuR binding to *SOD2* mRNA. Using HuR siRNA-mediated knock-down, we show that the presence of HuR is necessary for the increase in *SOD2* mRNA association with the heavy polyribosome fraction and SOD2 protein synthesis observed in anchorage-independence. Cellular detachment activates the stress-response protein kinase p38 MAPK, which is necessary for HuR-*SOD2* mRNA binding and optimal increases in SOD2 protein expression. These findings illustrate a novel post-transcriptional regulatory mechanisms of SOD2, enabling cells to rapidly increase their mitochondrial antioxidant capacity as an acute response to anchorage-independence.

Introduction

In vivo studies have demonstrated that increased antioxidant enzyme expression and small molecule antioxidant treatment promote the metastatic spread of melanoma and breast cancer cells [1, 2], suggesting that the maintenance of redox homeostasis is a key adaptation during metastasis. Manganese superoxide dismutase (SOD2) is an important mitochondrial antioxidant enzyme that resides in the mitochondrial matrix and is responsible for scavenging the majority of superoxide produced as a biproduct of respiration. SOD2 is often upregulated during tumor progression and it's expression is important for successful metastasis of cancer cells [3-8]. A key step during metastasis is a tumor cell's ability to survive in non-adherent conditions and to evade anchorage-independent cell death, known as anoikis. This process has been associated with an increased capacity of tumor cells to scavenge reactive oxygen species that are elevated in response to detachment [9, 10]. We previously demonstrated that epithelial ovarian cancer cells increase their mitochondrial antioxidant capacity after matrix detachment, by upregulating the transcription and activity of the deacetylase sirtuin 3 (SIRT3), and it's target protein SOD2 [6]. Both proteins conferred anoikis resistance and promoted transcoelomic spread of ovarian cancer cells *in vivo* [6].

SOD2 is a nuclear encoded protein responsive to stress-activated transcriptional regulation [7]. Nrf2 (encoded by *NFE2L2*), a major transcription factor responsive to oxidants, has been implicated in regulating increased SOD2 expression in tumor cells including breast and clear cell ovarian carcinomas [4, 11]. *SOD2* transcription can also be induced by the sirtuin regulated transcription factor Foxo3A [12], and by NF-κB, which has been shown to induce *SOD2* transcription in response to breast cancer cell matrix detachment [13]. Although much emphasis has been placed on the transcriptional mechanisms of *SOD2* expression, the impact of *SOD2* translational regulation remains less well established in tumor cells.

Posttranscriptional and translational regulatory mechanisms are crucial for fine-tuning of gene expression, and enabling rapid protein synthesis in response to specific cues. In particular, the interplay between mRNAs, miRNAs, and RNA-binding proteins has been implicated in the regulation of protein expression during cancer development and metastasis [14-16]. HuR (encoded by *ELAVL1*) is one RNA-binding protein that has been implicated in the regulation of mRNAs that encode proteins involved in oncogenic signaling [17-19], anti-apoptotic mechanisms [20], cell cycle regulation [21, 22], and chemoresistance [23]. By binding to the AU- and U-rich elements (AREs) in the 3' UTR of target mRNAs, HuR exerts multiple functions, including RNA splicing, regulation of mRNA stability and translation [24]. Importantly, HuR cytoplasmic

translocation and mRNA binding is induced upon genotoxic or extracellular stress stimuli [21, 25], which suggests that HuR-dependent translation may be a critical stress adaptation utilized by cancer cells. HuR expression analyses across different malignancies, including ovarian cancer, shows that its expression and cytoplasmic accumulation correlates with advanced tumor stage and poor patient prognosis [26-29].

Using ovarian cancer cells as a model, we observed that SOD2 protein levels rapidly rise in response to matrix detachment, which preceded increases *SOD2* transcript expression. A transcriptome-wide RNA-binding analysis identified multiple HuR binding sites in the 3' UTR of *SOD2* mRNA [30]. However, the functional consequences of these sites and potential regulatory role of HuR in regulating *SOD2* mRNA translation in cancer cells have not been investigated. In the present work, we show that *SOD2* mRNA is a target of HuR binding and that the interaction of HuR with *SOD2* mRNA is enhanced and required for rapid *de novo* SOD2 protein synthesis after matrix detachment. Our study provides evidence for a novel mechanism of rapid SOD2 regulation in response to acute stress associated with anchorage-independence.

Results

SOD2 protein expression increases rapidly in response to anchorage independence.

To further assess the regulation of SOD2 in conditions of anchorage independence, we used ovarian cancer cell lines, as these tumor cells are prone to adapt to matrix detachment for transcoelomic metastasis in the peritoneal cavity and anchorage independent survival in ascites. SOD2 protein expression was assessed using ultra low attachment cell culture conditions, which revealed that SOD2 protein levels rapidly increase within 0.5 and 2 hours following cellular detachment of OVCA433 and OVCAR10 ovarian cancer cells, respectively (Fig 1A). Treatment with the protein synthesis inhibitor cycloheximide demonstrated that these increases in SOD2 likely represent newly synthesized SOD2 protein pools under anchorage independent culture conditions (Fig 1A). ^{35}S-Met/Cys incorporation assays showed global increases in protein synthesis immediately following detachment (Suppl. Fig 1A), and subsequent immunoprecipitation of SOD2 demonstrated 1.8-fold (OVCA433) and 2.4-fold (OVCAR10) increases in ^{35}S-Met/Cys incorporation into the SOD2 protein compared to attached conditions (Fig 1B, Suppl. Fig 1B-C). These changes were again abrogated by cycloheximide treatment, verifying increased SOD2 protein synthesis in short-term anchorage independent conditions. To focus on the newly synthesized pool of SOD2, we further assessed changes in SOD2 levels within the cytosolic fraction of cells following matrix detachment. Subcellular fractionation demonstrated an average 4.7-fold increase in OVCA433 cytosolic SOD2 expression after 0.5 hour of detachment compared to attached cells, while a 1.5-fold increase was observed after 2 hours in anchorage-independent conditions in OVCAR10 cells (Fig 1C). Increases in *SOD2* mRNA levels trailed the surges in SOD2 protein expression in OVCA433 cells, suggesting that the rapid rise in SOD2 protein levels following detachment is likely independent of increases in transcription in this cell line (Fig 1D).

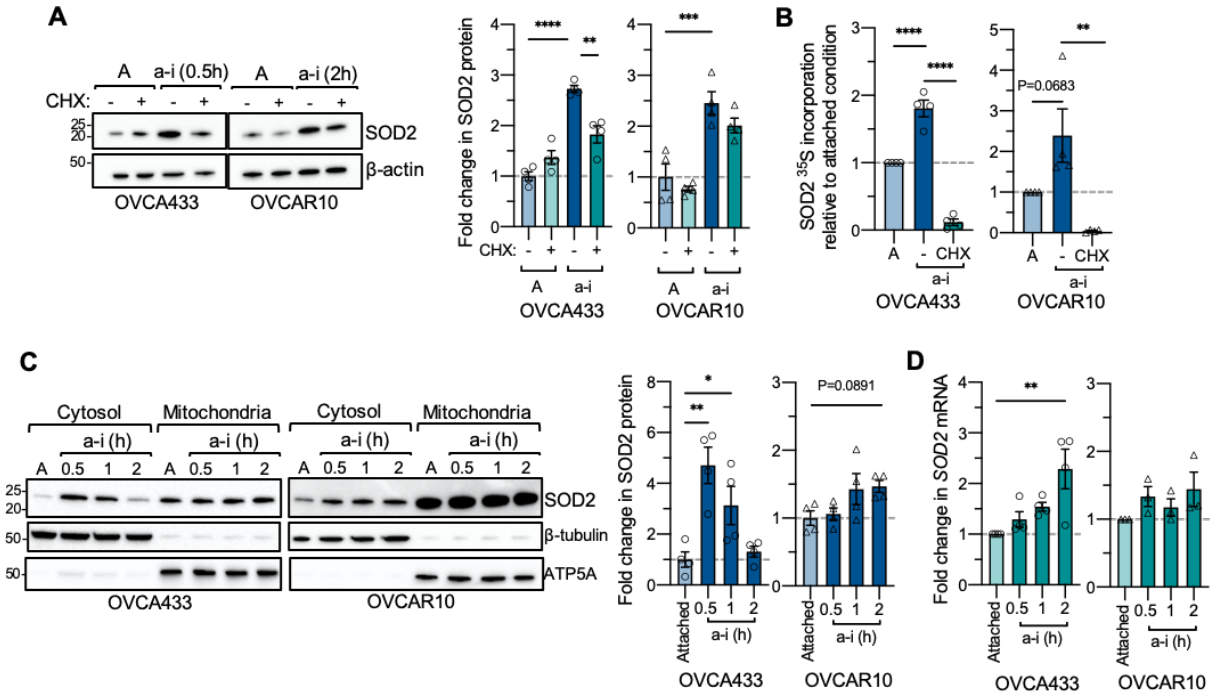

Figure 1.

A. Total SOD2 protein levels were assessed by immunoblotting in response to culture in anchorage-independent conditions and protein synthesis inhibited by cycloheximide (CHX, 20 µg/mL; *n*=4, one-way ANOVA, *P*<0.0001, Tukey's multiple comparison test *P<0.05; **P<0.01).

B. ^{35}S-Met/Cys incorporation assay followed by SOD2 IP (Suppl. Fig 1B&C), demonstrates increased ^{35}S-Met/Cys incorporation into SOD2 under anchorage independence compared to attached cells, which is abrogated in the presence of cycloheximide (*n*=4, one-way ANOVA, OVCA433 *P*<0.0001, OVCAR10 *P*=0.0057, Tukey's multiple comparison test **P<0.01; ****P<0.0001).

C. The cytosolic SOD2 protein pool increases rapidly in response to anchorage-independence (a-i), compared to attached culture conditions (A). Cells were maintained for indicated times in ULA plates and SOD2 protein expression assessed following cellular fractionation and immunoblotting. Fold change in SOD2 cytosolic protein expression in response to anchorage-independent (a-i) culture was quantified using densitometry, normalized to β-tubulin loading control and expressed relative to attached (A) culture conditions (*n*=4, one-way ANOVA, OVCA433 *P*=0.0015, OVCAR10 *P*=0.0744, Dunnett's multiple comparison test *P<0.05; **P<0.01).

D. Fold change in *SOD2* mRNA in response to short term anchorage-independent culture was assessed using semi-quantitative real time RT-PCR (*n*=3-4, one-way ANOVA, OVCA433 *P*=0.0069, OVCAR10 *P*=0.2946, Dunnett's multiple comparison test *P<0.05; **P<0.01).

To confirm that the increase in SOD2 expression is due to *de novo* protein synthesis in OVCA433 cells, ribosome-mediated mRNA translation was assessed using polyribosome profiling. Following centrifugation, sucrose gradients were separated into four fractions and RNA was isolated from each fraction. Fraction 1 contains mRNAs not associated with ribosomes, fraction 2 contains mRNAs associated with one or two ribosomes, fraction 3 contains mRNAs associated with 3-6 ribosomes (referred to hereafter as 'light polysomes'), and fraction 4 contains mRNAs associated with >6 ribosomes (referred to as 'heavy polysomes'; Fig 2A). In attached conditions, *SOD2* mRNA was primarily found in fractions 2 and 3 (Fig 2B&C), suggesting that *SOD2* is translated at a constitutive level in this condition, which is evident by ready detection of SOD2 protein by western blotting. In anchorage independent conditions the relative proportion of *SOD2* mRNA shifted to fractions 3 and 4. In particular, anchorage independent cells showed a significant shift towards an enrichment of *SOD2* mRNA in the heavy polyribosome fraction 4 (Fig 2B&C), demonstrating a larger number of ribosomal units associated with *SOD2* mRNA and an increase in *SOD2* mRNA translation in anchorage independent conditions. As a point of comparison, the mRNA of the nutrient stress response protein ATF4 also shifted into fraction 4 in response to anchorage-independence (Supp Fig 2).

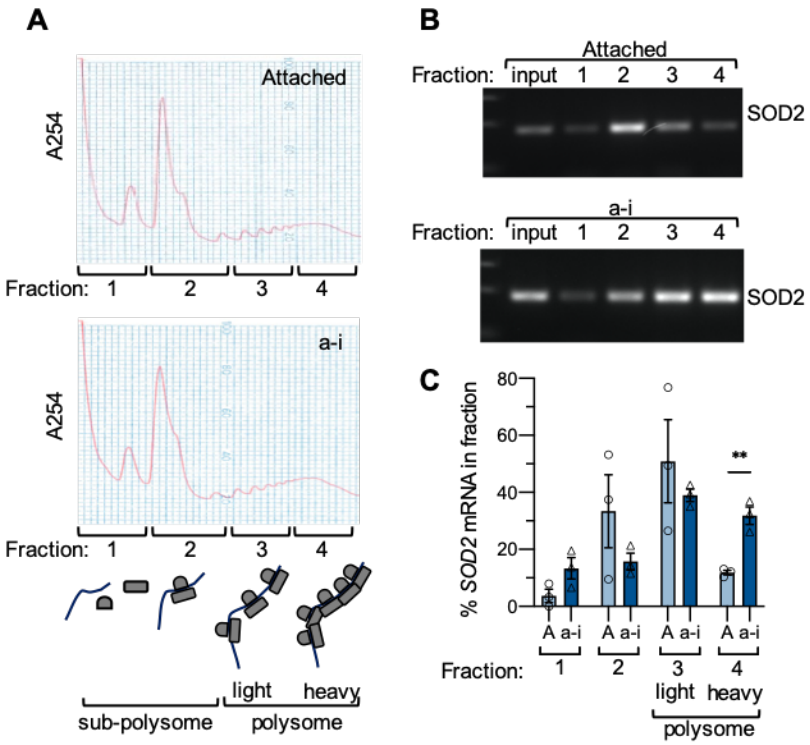

Figure 2.

A. Polyribosome profiling was carried out after OVCA433 cells were cultured in attached (A) and anchorage independent (a-i) conditions (0.5 h) and analyzed by sucrose density gradient centrifugation. Four fractions were collected as indicated, and RNA extracted.
B. Polyribosome profiling demonstrates an increase in the percentage of *SOD2* mRNA in the heavy polysomal fraction 4 in response to anchorage independence. Representative image of *SOD2* RT-PCR from RNA isolated from each polysomal fraction.
C. Quantification of relative *SOD2* mRNA levels in each fraction demonstrates increased proportion of *SOD2* in fraction 4 following culture in anchorage independent conditions (n=3; t-test, $^{**}P<0.01$).

HuR accumulates in the cytosol and binds *SOD2* mRNA in response to anchorage-independence

Regulation of gene expression at the translational level is mediated by the interplay between mRNAs and RNA binding proteins. HuR (encoded by the gene *ELAVL1*) is a major RNA binding protein that has been implicated with alternative splicing, mRNA stability, and translation during stress conditions [21, 25, 31]. HuR recognizes and binds to AU-/ U-rich elements in target mRNA transcripts. Analysis of HuR RNA binding by screening of publicly available RNA immunoprecipitation sequencing (RIP-seq; ENCODE: ENCSR000CWW, ENCSR000CWZ) [32, 33] and photoactivatable ribonucleoside-enhanced crosslinking and immunoprecipitation (PAR-CLIP; GSE29943) [30] transcriptome-wide data sets revealed that the *SOD2* mRNA contains multiple binding sites for HuR within 3.5 kb downstream of the STOP codon in the *SOD2* 3' UTR (Fig 3A, Supp Fig 3A). While the 5' UTR of *SOD2* is less than 75 bp in length, the complete *SOD2* 3' UTR spans 13,424 bp (Fig 3A, Variant 1: NM_000636). *SOD2* transcripts with variable 3' UTR lengths have previously been reported (Suppl Fig 3A) (Chaudhuri *et al*, 2012; Church, 1990). Using RT-PCR we confirmed that OVCA433 and OVCAR10 cells express the longer 3.4 kb 3' UTR containing the majority of HuR sites identified (Suppl Fig 3B).

To examine if HuR regulates SOD2 protein expression in response to anchorage independence, cytosolic translocation of HuR in response to culture in ULA plates was first determined. Concurrent with the increases in SOD2 protein expression, HuR cytosolic protein levels increased significantly in OVCA433 within 0.5 hours of anchorage independence and within 2 hours in OVCAR10 cells (Fig 3B). We next investigated if HuR binds to *SOD2* mRNA in anchorage independent conditions using ribonucleoprotein immunoprecipitation to capture the HuR-bound mRNAs (Fig 3C, Supp Fig 3C). *SOD2* mRNA was more readily detected by PCR in HuR immunoprecipitates from OVCA433 and OVCAR10 cells cultured under anchorage independence compared to attached conditions (Fig 3C), indicating that matrix detachment causes the binding of HuR to *SOD2* mRNA.

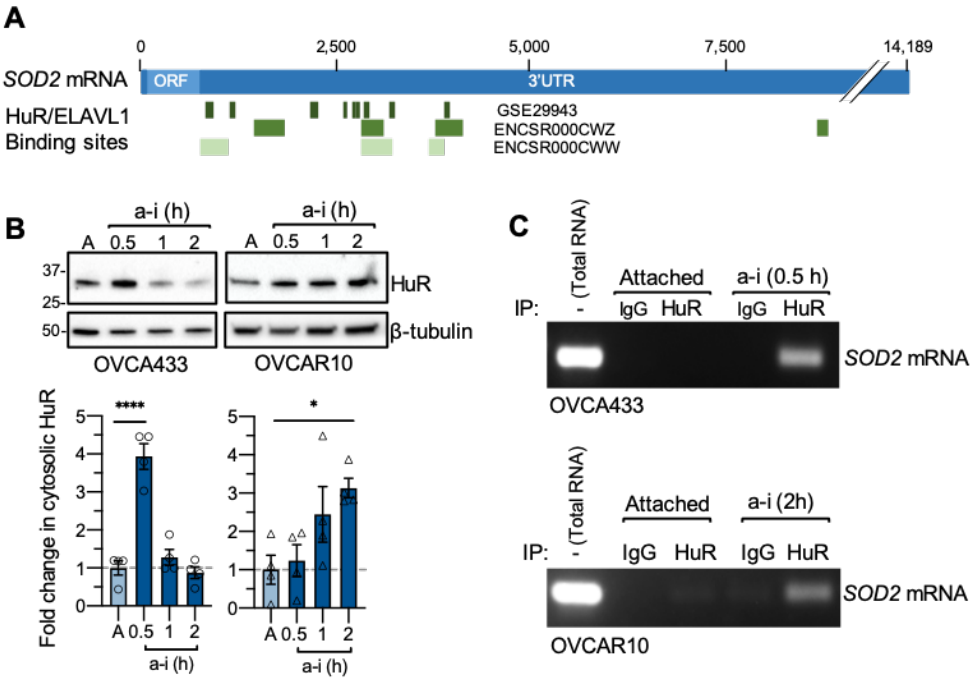

168

Figure 3.

A. HuR/ELAVL1 binding profiles on the *SOD2* mRNA was assessed using ENCODE RIP-seq data sets ENCSR000CWW and ENCSR000CWZ, and PAR-CLIP data set GSE29943.
B. HuR accumulates in the cytosol in response to anchorage-independence (n=4, one-way ANOVA, OVCA433 P<0.0001, OVCAR10 P=0.0248, Dunnett's multiple comparison test **P<0.01; ***P<0.001).
C. Anchorage-independence induces HuR binding to *SOD2* mRNA, as assessed by Ribonucleoprotein Immunoprecipitation and *SOD2* RT-PCR following OVCA433 culture in attached or anchorage independent conditions (a-i, OVCA433: 0.5h; OVCAR10: 2h).

169

Since HuR binds to *SOD2* mRNA shortly after matrix detachment, we investigated the functional consequences of the HuR-*SOD2* mRNA interaction using siRNA mediated knockdown of HuR/*ELAVL1*. An established function of HuR as a stress response RNA binding protein is its role in mRNA stabilization within the cytosol [20, 34]. To determine if HuR has an effect on *SOD2* mRNA stability, we treated ovarian cancer cells with the transcription inhibitor actinomycin D. Compared to attached conditions, anchorage independence did not significantly alter *SOD2* mRNA stability in OVCA433 cells (Fig 4A), while decreased *SOD2* mRNA stability in anchorage independence was observed in OVCAR10 cells compared to attached conditions (Fig 4B, two-way ANOVA, P=0.0104), indicating that these cells differ in mechanisms regulating *SOD2* mRNA stability. However, HuR knockdown did not significantly alter *SOD2* mRNA levels in response to actinomycin D treatment in anchorage independent or attached culture conditions (Fig 4), suggesting that increased binding of HuR to *SOD2* mRNA does not influence *SOD2* mRNA stability.

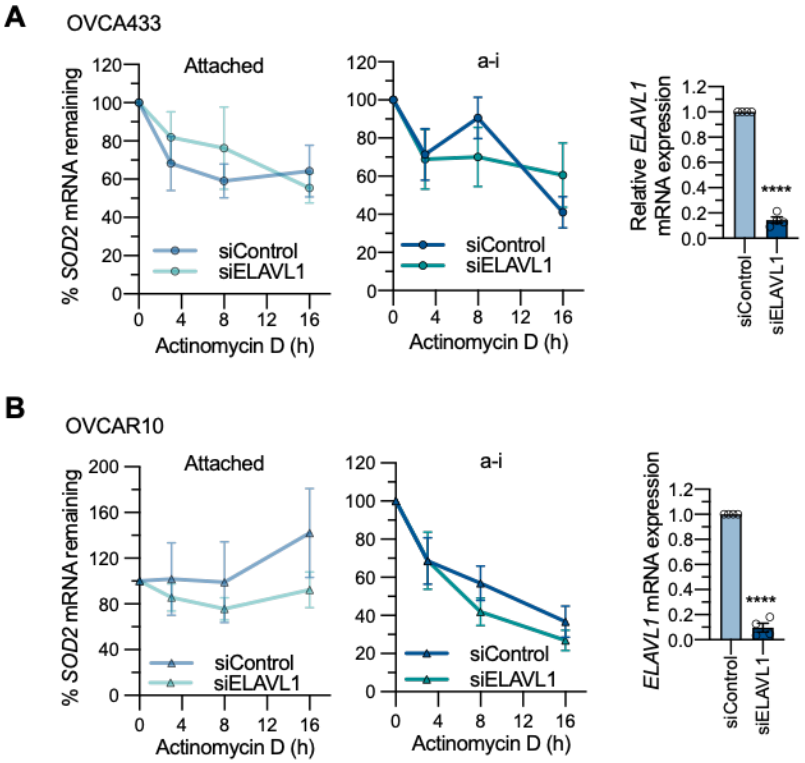

Figure 4.
HuR knock-down does not affect *SOD2* mRNA stability in attached or anchorage-independent conditions, as determined by Actinomycin D treatment (*n*=4; two-way ANOVA: ns). HuR knock-down was assessed by semi quantitative real time RT-PCR (t-test, ****$P<0.0001$). A: OVCA433 B: OVCAR10.

HuR enhances *SOD2* mRNA translation under anchorage independence

We next tested if HuR is necessary for enhanced *SOD2* mRNA translation in anchorage independence. Following siRNA-mediated HuR (ELAVL1) knockdown, matrix detachment-induced increases in SOD2 cytosolic protein levels were significantly abrogated (Fig 5A). To further demonstrate that increased SOD2 protein synthesis in anchorage independent cells is HuR-dependent, polyribosome profiling following siRNA mediated HuR knock-down was carried out (Fig 5B). In response to culture in anchorage independent conditions, *SOD2* mRNA shifted towards the heavy polyribosome fraction (fraction 4) in OVCA433 cells transfected with a scramble control siRNA (Fig 5C), as demonstrated above in un-transfected cells (Fig 2). HuR knockdown abrogated this shift of *SOD2* mRNA to the heavy polyribosomal fraction, and anchorage independent cultured cells lacking HuR displayed a similar distribution of *SOD2* mRNA in polysomal fractions compared to attached cells (Fig 5C). There was no difference in *SOD2* mRNA abundance in the subpolysome fractions (fractions 1 & 2) following HuR knock-down, indicating that a loss of HuR does not lead to a complete loss of *SOD2* mRNA translation. This suggests that the primary function of HuR is to enhance *SOD2* translation in response to anchorage independence, boosting SOD2 protein levels under these conditions.

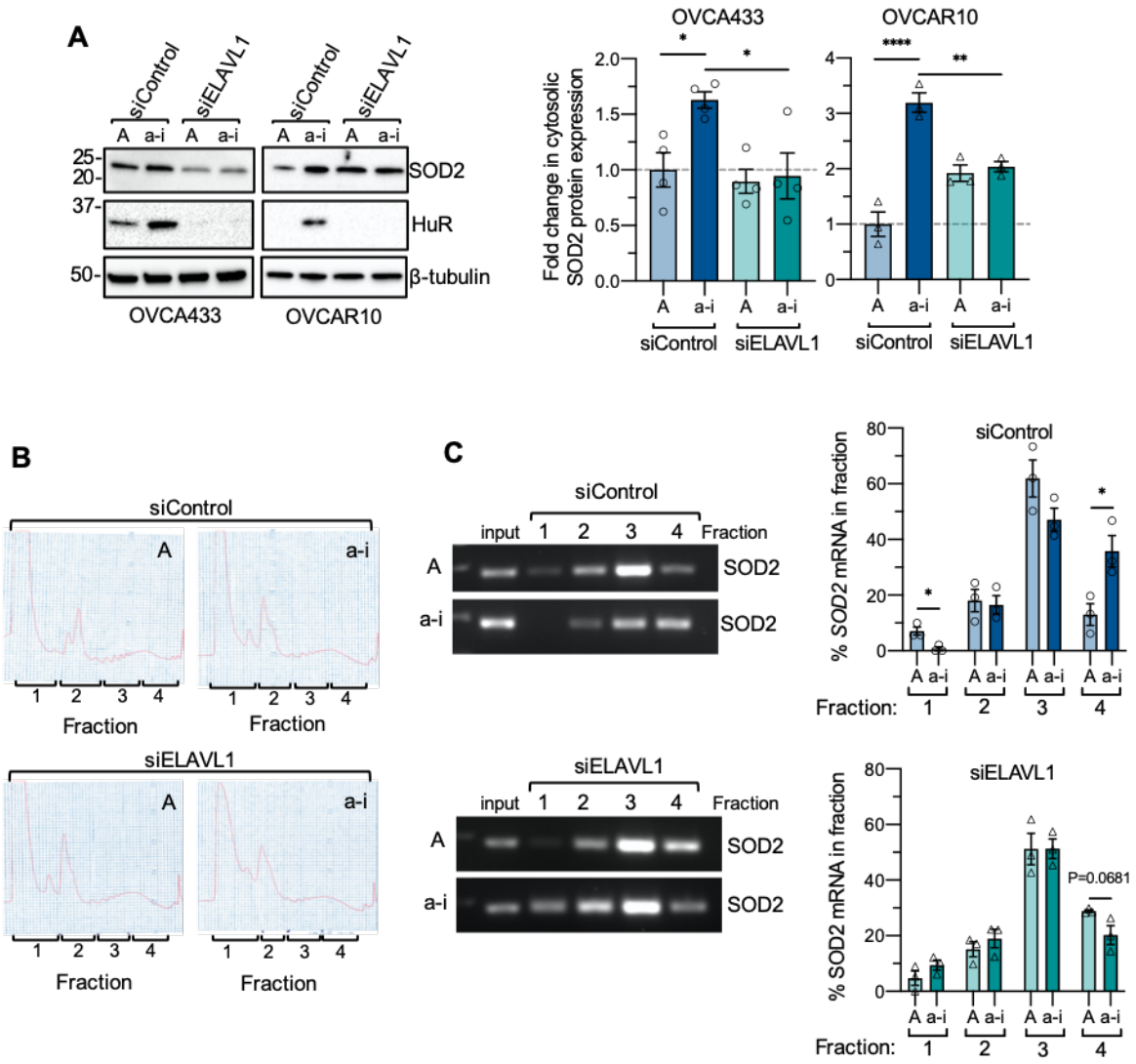

202

Figure 5.

A. HuR/ELAVL1 knock-down abrogates increases in cytosolic SOD2 expression in short term anchorage-independence (a-i, OVCA433 0.5 h; OVCAR10 2 h) compared to attached cultures (A; *n*=3-4, one-way ANOVA, OVCA433 *P*=0.012, OVCAR10 *P*=0.0001; Tukey's multiple comparison test **P*<0.05, ***P*<0.01, *****P*<0.0001).

B. Polysome profiles of OVCA433 cells cultured in attached (A) and anchorage independent (a-i, 0.5 h) conditions following siRNA-mediated HuR/ELAVL1 knockdown.

C. HuR knock-down abrogates a shift of *SOD2* mRNA into fraction 4 in response to anchorage independence (a-i). Representative image of *SOD2* RT-PCR from polyribosome fractions and quantification of relative *SOD2* mRNA levels in each fraction shown (*n*=3; t-test, **P*<0.05).

203

Inhibition of p38 MAPK activation in response to anchorage independence abrogates increases in SOD2 protein expression and HuR-*SOD2* mRNA binding.

HuR can be activated in response to cellular stress *via* the p38 MAPK kinase signaling pathway [35, 36]. p38 MAP kinase signaling is frequently activated and uncoupled from pro-apoptotic pathways in cancer cells to ensure cell survival under stress conditions and during metastatic progression [37-39]. An increase in p38 MAPK phosphorylation was previously reported in ovarian cancer cell lines cultured in long-term anchorage independence (24-48 h) [40]. We were able to show that short-term anchorage independence (0.5-2 h) was sufficient to also increase p38 MAPK phosphorylation in OVCA433 and OVCAR10 cell lines (Fig 6A). To determine if the p38 MAPK pathway is involved in the observed increases in cytosolic SOD2 protein expression during this time, cells were treated with the p38 MAPK inhibitor, SB203580. SB203580 inhibited the phosphorylation of the p38 target MAPKAPK2 and abrogated the increases in SOD2 protein expression observed in anchorage independent conditions (Fig 6B). In addition, the formation of the HuR-*SOD2* mRNA complex was monitored in the presence of p38 MAPK inhibition. Similar to Fig 3, anchorage independent conditions increased *SOD2* mRNA binding to HuR, while treatment with SB203580 decreased this interaction (Fig. 6C). The above demonstrates a link between p38 MAPK signaling, HuR binding to the *SOD2* mRNA and SOD2 expression in response to cellular detachment. p38 MAPK has previously been shown to phosphorylate Thr 118 of HuR [25, 41]. In the absence of a commercially available phospho-Thr118 HuR specific antibody we were unable to successfully demonstrate that anchorage independence or p38 MAPK inhibition influences phosphorylation of HuR using HuR IP and a pan phospho-Thr antibody (data not shown). In OVCAR10 cells, p38 MAPK inhibition resulted in slight decreases in cytosolic HuR accumulation in response to anchorage-independence, while this could not be consistently observed in OVCA433 cells (Fig. 6D). The above data suggest that p38 signaling primarily regulates HuR *SOD2* mRNA binding rather than HuR cellular localization.

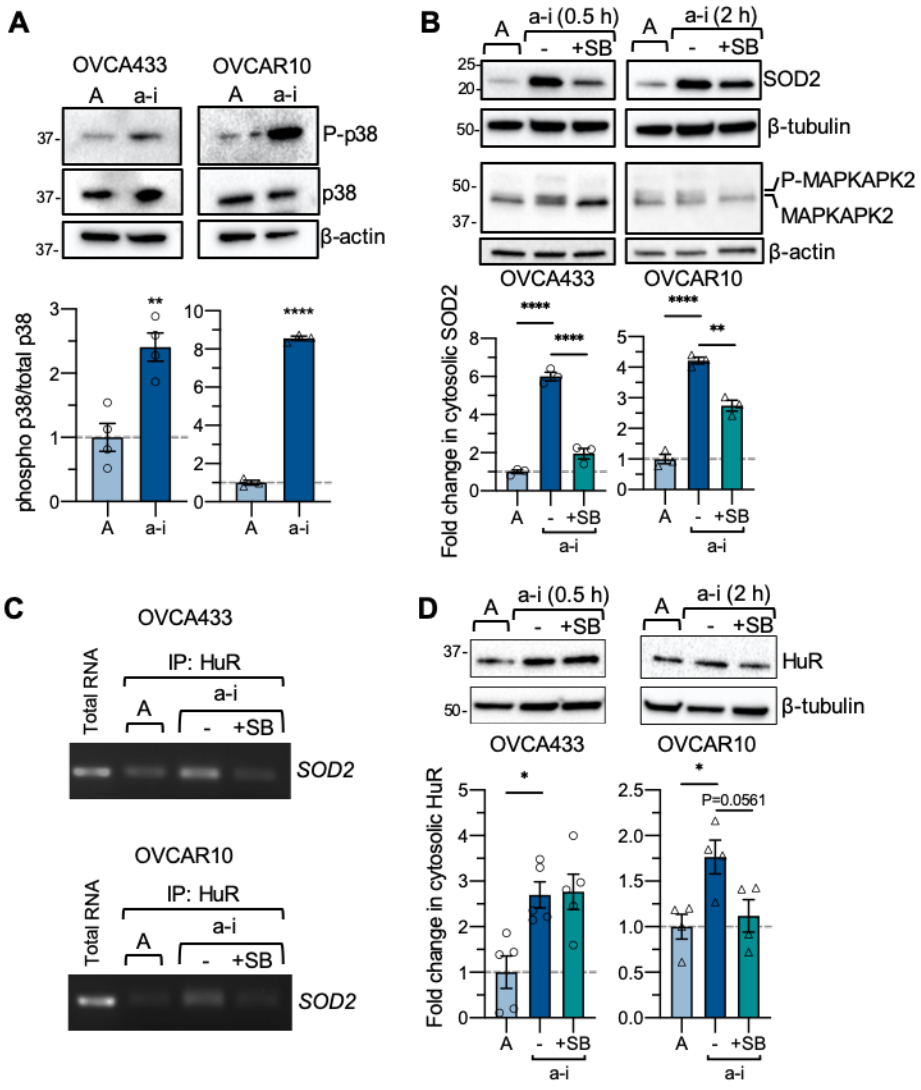

Figure 6.

A. p38 MAPK (Thr180/Tyr182) phosphorylation is induced in response to culture in anchorage-independent culture conditions (a-i OVCA433 0.5 h, OVCAR10 2 h; n=4, T-test, ***P*<0.01, *****P*<0.0001).
B. p38 MAPK inhibition abrogates a-i induced increases in SOD2 expression (n=3, one-way ANOVA *P*<0.0001, Tukey's multiple comparison test ***P*<0.01, *****P*<0.0001).
C. p38 MAPK inhibition abrogates HuR binding to *SOD2* mRNA in anchorage-independence, as assessed by RNA immunoprecipitation.
D. Effects of p38 MAPK inhibition on cytosolic HuR levels (n=4-5, one-way ANOVA, OVCA433 *P*=0.0053, OVCAR10 *P*=0.0221, Tukey's multiple comparison test ***P*<0.01, *****P*<0.0001).

Discussion

Recent studies have highlighted that tumor cells need an adequate antioxidant system to deal with intrinsic and extrinsic increases in ROS associated with metastatic progression [1, 2, 6]. Tumor cells must therefore readily adapt to increase their antioxidant capacity at the transcriptional and post-transcriptional levels. In line with these findings, we previously showed that SIRT3-mediated deacetylation of SOD2 drives transcoelomic metastasis by increasing mitochondrial antioxidant capacity in anchorage-independent ovarian cancer cells [6]. The present work demonstrates that translation contributes to the regulation of SOD2 during early-stage anchorage independence. We found that detachment induces *SOD2* mRNA translation in a HuR-dependent manner, and that the p38 pathway contributes to HuR-*SOD2* mRNA binding.

Aberrant HuR expression has been reported in several malignancies, including ovarian cancer [26-28]. HuR's pro-tumorigenic function involves selective mRNA binding, mRNA stabilization and/or increased translation of target mRNAs. Previously identified HuR targets include mRNAs encoding pro-survival and anti-apoptotic proteins, such as Bcl-2 , proteins that support invasion and metastasis, and angiogenic factors, such as VEGF [20, 22, 35, 42, 43]. HuR knock-down decreased glioma cell survival in anchorage independence, and it was found that HuR knock-down increased apoptosis and decreased *Bcl-2* mRNA stability and protein expression [20]. Moreover, HuR regulation can interplay with miRNAs to further fine tune expression in cancer, as has been demonstrated in ovarian cancer with miR-200c [44]. This growing repertoire of cancer-related mRNAs regulated by HuR suggests a critical role of this RNA binding protein in cancer cells. Our data identify SOD2, an important antioxidant enzyme for the maintenance of mitochondrial redox homeostasis, as a novel HuR target during early-stages of anchorage-independence.

HuR is a predominantly nuclear protein which translocates to the cytoplasm upon extrinsic or intrinsic stimuli and stress signals. Depending on the location of target HuR aminoa acid residues, posttranslational modifications of HuR by different signaling pathways have been shown to affect its RNA binding affinity, nucleo-cytoplasmic shuttling, and HuR protein stability [24]. Among different kinases activated during stress, p38 MAPK-dependent phosphorylation on Thr118 induces cytoplasmic accumulation of HuR and increased p21 mRNA binding after exposure to ionizing radiation [25] and enhanced mRNA binding upon IL-1β treatment [41]. Consistent with these previous findings, we found that stress associated with matrix detachment activated p38 MAPK (Fig 6). Importantly, activation of the p38 MAPK pathway increased SOD2 cytosolic protein expression under anchorage independence and we found that the association

of HuR with *SOD2* mRNA was also p38 MAPK-dependent (Fig 6). It remains to be determined whether HuR is phosphorylated on Thr118 in anchorage independent cells, or if p38 MAPK indirectly activates HuR to bind *SOD2* mRNA. Although p38 has previously been implicated in cytosolic shuttling of HuR in response to stress [35, 36, 45], cytosolic HuR accumulation was not greatly affected by the p38 MAPK inhibition in anchorage independence, unlike *SOD2* mRNA binding (Fig 6). This raises the possibility that additional stress signaling pathways could contribute to the HuR nucleo-cytoplasmic shuttling observed following matrix detachment, and points to the previously reported multifaceted and context dependent regulation of HuR. For example, post-translational modifications of residues within HuR's RNA recognition motifs leads primarily to changes in HuR RNA binding, while phosphorylation of the hinge region affects nuclear to cytoplasmic shuttling [46, 47]. Threonine 118, the target of p38 signaling, is located in one of the RNA recognition motifs [25], which may explain why the activation of p38 signaling in anchorage-independence primary affects HuR Sod2 mRNA binding. The exploration of additional HuR mRNA targets following matrix detachment and mechanisms linking the p38 MAPK pathway to HuR activation require further investigation to unveil novel stress response translational pathways under conditions of anchorage independence.

While the transcriptional regulation of antioxidant enzymes has been studied widely in the context of antioxidant response elements and stress response transcription factors, such as Nrf2, fewer studies have focused on translational regulation of these enzymes. In earlier work, the presence of an un-identified redox-sensitive *SOD2* mRNA binding protein was reported in rat lung extracts [48]. Further analysis identified that RNA binding occurred at a cis-regulatory region located 111 bp downstream of the stop codon in the rat *SOD2* mRNA [49]. The 3' UTR of human *SOD2* mRNA shares ~75% homology with the rat 3' UTR. Based on sequence comparison, the previously identified rat RNA protein binding region partially overlaps with the first HuR binding sites from PAR-CLIP analysis (Fig 3A) [30, 49], suggesting that this region could be an important RNA regulatory domain of *SOD2* mRNA. Among the different *SOD2* mRNA splice variants, different 3' UTRs have been reported (Supp Fig 3A). Variant 2 (NM_001024465) has a short 3' UTR composed of a spliced region that excludes the majority of the HuR sites identified. Variant 1 (NM_000636) has been annotated to contain a 13.4 kb 3' UTR. However, past studies have shown that the two most common *SOD2* transcripts contain either a short 240 bp or a 3,439 bp segment of this 3' UTR, which arise from use of a proximal and distal polyadenylation site, respectively (Supp Fig 3A) [50, 51]. Interestingly, Chaudhuri *et al.* reported that the expression of these two *SOD2* transcripts is altered between quiescent and proliferating cells, with the shorter transcript being associated with quiescence and increased protein expression [50]. Moreover,

298 radiation increased levels of the shorter *SOD2* transcript levels of the 1.5 kb MnSOD transcript,
299 with expression of the longer form remaining unaltered [50]. The mechanisms for this radiation
300 induced increase in the short 3' UTR transcript remain unclear. However, we predict that it is likely
301 not HuR-dependent, as only the longer 3.4 kb 3' UTR contains the majority of identified HuR
302 binding sites. We verified that ovarian cancer cells used in the present work express the transcript
303 containing the longer 3' UTR (Supp Fig 3B). Further studies are needed to determined if and how
304 these alternate 3' UTR *SOD2* transcripts are regulated in response to different sources of stress,
305 and how their transcription co-operates with translational regulation through the activation of cell-
306 specific RNA binding proteins, as well as the interplay with non-coding RNAs, such as miRNAs.
307 A screen for miRNA binding reveals that the *SOD2* mRNA contains potential binding sites for
308 miRNAs throughout the length of the 3' UTR. While most are located toward the far upstream
309 region, several overlap with identified HuR binding sites. Several studies have investigated the
310 role of miRNAs in regulating SOD2 expression and miRNAs identified that either positively or
311 negatively regulate SOD2 levels in cancer (reviewed in [7]). It remains to be investigated if
312 changes in miRNA binding further influence the regulation of *SOD2* mRNA translation in
313 anchorage-independence, and if this interplays with the regulation by HuR.

314 In conclusion, we show for the first time that *SOD2* mRNA is an HuR target in anchorage-
315 independent ovarian cancer cells. The present findings uncover a novel post-transcriptional stress
316 response mechanism by which tumor cells are able to rapidly increase the expression of SOD2
317 in response to anchorage-independence.

Materials and Methods:

Cell Culture and Reagents

OVCA433 and OVCAR10 cells were provided by Dr. Susan K. Murphy (Duke University) and Dr. Katherine Aird (Penn State University & University of Pittsburgh), respectively. OVCA433 and OVCAR10 were grown in RPMI1640 supplemented with 10% FBS at 37 ºC with 5% CO_2. STR profiling is carried out routinely to validate cell identity, which revealed at the commencement of this work that OVCAR10 cells share the same STR profile as NIH-OVCAR3 cells. It is unclear if the OVCAR10 cell line was initially derived from the same patient as OVCAR3, or if OVCAR10 cells represent a sub-line derived from OVCAR3 cells. The protein synthesis inhibitor cycloheximide (Sigma) was added at a concentration of 20 µg/mL in fully supplemented growth media. For mRNA stability assays, actinomycin D (Sigma) was added at 10 µg/mL. The p38 MAPK inhibitor SB203580 was used at a final concentration of 20 µM.

Cell culture in adherent and ultra-low attachment (ULA) conditions

For attached conditions, cells were plated in 150-mm dishes and grown to ~80% confluency. For anchorage independent cell culture, cells were trypsinized and seeded at a density (300,000 cells/2 mL media/well) in 6-well ULA (ultra-low attachment) plates (Corning: 3471) and collected at different time points for downstream analyses.

siRNA-mediated HuR/ELAVL1 knock-down

Cells were transfected with scramble non-targeting SMARTpool control (Dharmacon: D-001810-10-05) or HuR (ELAVL1)-specific SMARTpool siRNA oligonucleotides (Dharmacon: L-003773-00-0005) using Lipofectamine RNAiMAX (Invitrogen), and knock-down confirmed by western blotting.

Subcellular Fractionation

Cells in adherent and ULA plates were collected and the cell pellets were washed with ice-cold PBS. The cell pellets were processed as described in Sugiura *et al.* [52]. Briefly, cells were centrifuged and resuspended in 200-500 µl of ice-cold homogenization buffer (10 mM HEPES pH 7.4, 220 mM mannitol, 70 mM sucrose, Roche protease and phosphatase inhibitor cocktails). The

lysates were homogenized by several passages through 27-G needles. Lysates were centrifuged at 800 g for 10 min, followed by centrifugation of the supernatants at 2,500 g for 15 min at 4 ºC. The mitochondrial pellets were resuspended in homogenization buffer and the supernatants were centrifuged at 100,000g for 1 h at 4 ºC using a Beckman Coulter Optima MAX Ultracentrifuge. Post-centrifugation supernatants containing cytosolic fractions were transferred to new tubes and used for immunoblotting.

Immunoblotting

Protein concentrations were measured using the Pierce BCA protein assay kit. An equal amount of protein lysates was loaded onto 4-20% SDS-PAGE gels. Following electrophoresis, proteins were transferred to PVDF membranes. For detection of proteins, the membranes were incubated with the following antibodies overnight at 4 ºC: SOD2 (A-2, Santa Cruz: sc-133134, 1:500 dilution); β-tubulin (9F3, Cell Signaling Technology: 2128, 1:1,000 dilution), ATP5A (Abcam: ab14748, 1:1000 dilution), β-actin (Thermo: AM4302, 1:10,000 dilution), HuR/ELAVL1 (3A2, Santa Cruz: sc-5261, 1:500 dilution), Phospho-p38 MAPK (Thr180/Tyr182, Cell Signaling Technology: 9211, 1:1000 dilution), p38 MAPK (A-12, Santa Cruz Biotechnology: sc-7972, 1:1000 dilution), MAPKAPK-2 (Cell signaling technology: 3042, 1:1000 dilution). The blots were developed using SuperSignal West Femto Maximum Sensitivity Substrate (Thermo: 34096) after incubation with horseradish peroxidase (HRP)-conjugated secondary antibodies (Amersham Biosciences) for 1 h at RT.

Immunoprecipitation (IP)

1-1.5 mg of cell lysates were pre-cleared by incubating with 2 µg normal rabbit IgG (Cell Signaling Technology: 2729S) or normal mouse IgG (Millipore: 12-371) on a rotator for 1 h at 4 ºC followed by an additional 1 h incubation with protein A- (Thermo: 20333) or protein G- agarose beads (50 µL; Thermo: 20399) at 4 ºC. Following centrifugation at 3000g for 10 min supernatants were transferred to clean tubes and incubated with either IgG or primary antibodies overnight at 4 ºC. 50 µL of agarose beads were added to the lysates for 1-2 h at 4 ºC and the antibody-bead complexes were washed three times in IP lysis buffer and further processed for downstream assays.

379 ^{35}S Protein Radiolabeling

380 Cells in adherent and ULA plates were treated with EasyTag Express^{35}S Protein Labeling Mix
381 (Perkin Elmer: NEG772), using 40 µl ^{35}S (440 uCi) per 20 mL media in 150-mm dish, 4 µl ^{35}S (44
382 uCi) /2 mL media/ well in ULA plates, according to a protocol adapted from Gallagher *et al.*
383 (Gallagher *et al*, 2008). Following 2 h incubation in the presence of ^{35}S-L-methionine and ^{35}S-L-
384 cysteine (^{35}S-Met/Cys), cells were collected, washed with ice-cold PBS, and harvested using
385 RIPA buffer supplemented with protease and phosphatase inhibitors. The cell lysates were
386 rotated for 30 min at 4 ºC, centrifuged at 12,000 rpm for 30 min at 4 ºC and supernatants
387 transferred to new tubes. After pre-clearing, the lysates were incubated overnight with 2 µg of
388 normal rabbit IgG or SOD2 antibody (Abcam: Ab13533). Following SOD2 IP, the lysates were
389 resolved in SDS-PAGE gels. The SOD2 band in each lane was cut with a razor blade and weighed.
390 The bands were dissolved in 1 mL of 1X TGS running buffer overnight on a rocker at 4 ºC. Next
391 day, dissolved gel pieces were further heated for 20 min at 60 ºC. The dissolved radioactive
392 sample solutions were transferred to glass vials containing 10 mL of Opti-Fluor (Perkin Elmer) in
393 duplicate (500 µl per vial). Liquid scintillation counting was performed using a Beckman Coulter
394 Scintillation Counter. The readouts were normalized against the values from untreated samples.

395

396 Ribonucleoprotein Immunoprecipitation & RT-PCR

397 Cells were cultured in attached and anchorage independent conditions as described above.
398 Before harvesting cells, 0.3% formaldehyde was added for 10 min at 37 ºC for crosslinking
399 followed by addition of glycine (final concentration 0.25 M) for 5 min for quenching. RNP-IP was
400 performed as described in [23, 53] with modifications. Briefly, crosslinked cells were lysed in 500-
401 1,000 µl NT1 buffer (100 mM KCl, 5 mM $MgCl_2$, 10 mM HEPES, [pH 7.0], 0.5% Nonidet P40
402 [NP40], 1 mM dithiothreitol [DTT], 100 units/mL SUPERase·In RNase Inhibitor [Invitrogen:
403 AM2694], protease inhibitors [Thermo: 78429], 0.2% vanadyl ribonucleoside complexes [New
404 England Biolabs: S1402S]). After centrifugation of lysates at 16,000 g for 15 min, the supernatants
405 were used for IP with normal mouse IgG or HuR antibody. The antibody-bead mixtures were
406 washed several times with NT2 buffer (50 mM Tris-HCl [pH 7.4], 150 mM NaCl, 1 mM $MgCl_2$,
407 0.05% NP40, RNAse inhibitor, protease inhibitor). IP samples for RNA elution were incubated
408 with proteinase K (30 µg/100 µl NT2 buffer with 0.1% SDS) for 30 min at 60 ºC. RNA was extracted
409 using TRIzol, followed by cDNA synthesis (Quantabio: 95047) and *SOD2* RT-PCR using the
410 PrimeSTAR polymerase (Takara: R010A) with the following cycles: 98°C for 10 sec, 98°C for 10

sec + 60°C for 10 sec + 72°C for 20 sec X 35-38 cycles, followed by a final extension step at 72°C for 2 min. PCR products were analyzed by 2% agarose gel electrophoresis.

Polysome Profiling by Sucrose Density Gradient Centrifugation

Cells in adherent and ULA plates were incubated with cycloheximide (100 µg/mL) for 10 min at 37 ºC before harvesting and were washed twice with ice cold 1X PBS containing cycloheximide. The cells were homogenized in 500 µl lysis buffer (50 mM HEPES, 75 mM KCl, 5 mM $MgCl_2$, 250 mM sucrose, 100 ug/mL cycloheximide, 2mM DTT, 20 U/µl SUPERase·In RNase Inhibitor [Invitrogen: AM2694], 10% Triton X-100, 13% NaDOC) and polysome profiling carried out as previously described [54]. Lysates were placed on ice for 10 min and centrifuged at 3000 g for 15 min at 4 ºC. 500 µl supernatants were loaded on linear sucrose gradients ranging from 20% to 47% (10 mM HEPES, KCl 75 mM, 5 mM $MgCl_2$, 0.5 mM EDTA) and were separated by ultracentrifugation in a SW41 rotor at 34,000 rpm for 4 h 15 min at 4 ºC (Beckman Coulter). Subsequently, four sucrose fractions were collected using a UV/VIS absorbance detector. TRIzol reagent (Invitrogen) was added to each fraction for RNA isolation. Briefly, post-centrifugation at 3,200g for 20 min after addition of 1/5 volume of chloroform, the aqueous layer was transferred, and 1/2 volume of isopropanol was added for overnight precipitation at -20 ºC. RNA was pelleted by centrifugation at 4,640 rpm for 55 min at 4 ºC. RNA pellets were washed with 70% ethanol twice and dissolved in RNAse-free water. After cDNA synthesis and qPCR reactions, final PCR products were analyzed on 2% agarose gels.

Semi-quantitative real-time PCR

Total RNA was isolated by RNA isolation kit (Zymo Research: R2052) and used for cDNA synthesis (Quantabio: 95047) according to the manufacturer's instruction. cDNA was mixed with iTaq™ Universal SYBR® Green Supermix (BioRad) and the primers listed in Table 1. Semi-quantitative real time RT-PCR was carried out using a BioRad qRT-PCR machine (BioRad), data normalized to the geometric mean of four housekeeping genes (Table 1), and expressed as fold-change in expression using the $2^{-\Delta\Delta CT}$ formula.

Table1: Primers used for RT-PCR and semi-quantitative real time PCR.

Primer	Sense	Antisense
SOD2 CDS	5'-TCCACTGCAAGGAACAACAG-3'	5'-CGTGGTTTACTTTTTGCAAGC-3'
SOD2 3'UTR-A	5'-ATAATGCTGGGGTGAGCAAC-3'	5'-GCTGAGGTGGGACAATCACT-3'
SOD2 3'UTR-B	5'-TGTGTATGCATGCTTGTGGA-3'	5'CCACCTTGCCCGTCTATTTA-3'
ATF4	5'- TGTCCTCCACTCCAGATCAT	5'-GGCTCATACAGATGCCACTATC-3'
ELAVL1	5'-CGCAGAGATTCAGGTTCTCC-3'	5'-CCAAACCCTTTGCACTTGTT-3'
Housekeeping genes:		
GAPDH	5'-GAGTCAACGGATTTGGTCGT-3'	5'-TTGATTTTGGAGGGATCTCG-3'
18S	5'-AGAAACGGCTACCACATCCA-3'	5'- CACCAGACTTGCCCTCCA-3'
HPRT1	5'-TGACCTTGATTTATTTTGCATACC-3'	5'-CGAGCAAGACGTTCAGTCCT-3'
TBP	5'-TTGGGTTTTCCAGCTAAGTTCT-3'	5'-CCAGGAAATAACTCTGGCTCA-3'

Live/dead staining

Live and dead cell fractions of cells cultured for 2 h in anchorage independence was assessed by staining with 4 μM Calcein AM and 4 μM ethidium homodimer (in PBS; Sigma) to visualize live and dead cells, respectively. Cells were exposed to both dyes for 30 min at 37 ºC, followed by imaging on a Keyence BZ-X700 fluorescence microscope. The percentage of live and dead cells were quantified using Image J.

Statistical Analysis

All data are representatives of at least three independent experiments. Data are presented as mean ± SEM with individual replicate values superimposed. Statistical analysis was performed using GraphPad Prism Software v9, with statistical tests chosen based on experimental design, as described in figure legends.

Acknowledgements

The authors would like to thank Ms. Sara Shimko and Lydia Kutzler for technical assistance. This work was supported by the U.S. National Institutes of Health grants R01CA242021 (N.H.) and R01CA230628 (N.H. & K.M.).

Author contributions

Y.S.K. designed the conceptual framework and experiments of the study, carried out the majority of the experiments and data analysis, prepared the figures and wrote the manuscript. J.E.W., P.T., Z.J. and A.E. assisted with experimental execution, and manuscript editing. K.M. and S.R.K. contributed to experimental design, data interpretation and manuscript editing. N.H. supervised and conceived the study, contributed to experimental design, assisted in data analysis, and assisted in writing and editing of the manuscript.

Conflict of interest

The authors have no conflicts of interest.

References

1. Davison, C.A., et al., *Antioxidant enzymes mediate survival of breast cancer cells deprived of extracellular matrix.* Cancer Res, 2013. **73**(12): p. 3704-15.

2. Piskounova, E., et al., *Oxidative stress inhibits distant metastasis by human melanoma cells.* Nature, 2015. **527**(7577): p. 186-91.

3. Connor, K.M., et al., *Manganese superoxide dismutase enhances the invasive and migratory activity of tumor cells.* Cancer Res, 2007. **67**(21): p. 10260-7.

4. Hart, P.C., et al., *Caveolin-1 regulates cancer cell metabolism via scavenging Nrf2 and suppressing MnSOD-driven glycolysis.* Oncotarget, 2016. **7**(1): p. 308-22.

5. Hemachandra, L.P., et al., *Mitochondrial Superoxide Dismutase Has a Protumorigenic Role in Ovarian Clear Cell Carcinoma.* Cancer Res, 2015. **75**(22): p. 4973-84.

6. Kim, Y.S., et al., *Context-dependent activation of SIRT3 is necessary for anchorage-independent survival and metastasis of ovarian cancer cells.* Oncogene, 2020. **39**(8): p. 1619-1633.

7. Kim, Y.S., et al., *Insights into the Dichotomous Regulation of SOD2 in Cancer.* Antioxidants (Basel), 2017. **6**(4).

8. Hempel, N., P.M. Carrico, and J.A. Melendez, *Manganese superoxide dismutase (Sod2) and redox-control of signaling events that drive metastasis.* Anticancer Agents Med Chem, 2011. **11**(2): p. 191-201.

9. Jiang, L., et al., *Reductive carboxylation supports redox homeostasis during anchorage-independent growth.* Nature, 2016. **532**(7598): p. 255-8.

10. Schafer, Z.T., et al., *Antioxidant and oncogene rescue of metabolic defects caused by loss of matrix attachment.* Nature, 2009. **461**(7260): p. 109-13.

11. Konstantinopoulos, P.A., et al., *Keap1 mutations and Nrf2 pathway activation in epithelial ovarian cancer.* Cancer Res, 2011. **71**(15): p. 5081-9.

12. Kenny, T.C., et al., *Selected mitochondrial DNA landscapes activate the SIRT3 axis of the UPR(mt) to promote metastasis.* Oncogene, 2017. **36**(31): p. 4393-4404.

13. Kamarajugadda, S., et al., *Manganese superoxide dismutase promotes anoikis resistance and tumor metastasis.* Cell Death Dis, 2013. **4**: p. e504.

14. Audic, Y. and R.S. Hartley, *Post-transcriptional regulation in cancer.* Biol Cell, 2004. **96**(7): p. 479-98.

15. van Kouwenhove, M., M. Kedde, and R. Agami, *MicroRNA regulation by RNA-binding proteins and its implications for cancer.* Nat Rev Cancer, 2011. **11**(9): p. 644-56.

16. Wurth, L. and F. Gebauer, *RNA-binding proteins, multifaceted translational regulators in cancer.* Biochim Biophys Acta, 2015. **1849**(7): p. 881-6.

17. Epis, M.R., et al., *The RNA-binding protein HuR opposes the repression of ERBB-2 gene expression by microRNA miR-331-3p in prostate cancer cells.* J Biol Chem, 2011. **286**(48): p. 41442-54.

18. Mazan-Mamczarz, K., et al., *Post-transcriptional gene regulation by HuR promotes a more tumorigenic phenotype.* Oncogene, 2008. **27**(47): p. 6151-63.

19. Wang, J., et al., *Multiple functions of the RNA-binding protein HuR in cancer progression, treatment responses and prognosis.* Int J Mol Sci, 2013. **14**(5): p. 10015-41.

20. Filippova, N., et al., *The RNA-binding protein HuR promotes glioma growth and treatment resistance.* Mol Cancer Res, 2011. **9**(5): p. 648-59.

21. Lal, S., et al., *HuR posttranscriptionally regulates WEE1: implications for the DNA damage response in pancreatic cancer cells.* Cancer Res, 2014. **74**(4): p. 1128-40.

22. Wang, W., et al., *HuR regulates cyclin A and cyclin B1 mRNA stability during cell proliferation.* EMBO J, 2000. **19**(10): p. 2340-50.

23. Raspaglio, G., et al., *HuR regulates beta-tubulin isotype expression in ovarian cancer.* Cancer Res, 2010. **70**(14): p. 5891-900.

24. Abdelmohsen, K. and M. Gorospe, *Posttranscriptional regulation of cancer traits by HuR.* Wiley Interdiscip Rev RNA, 2010. **1**(2): p. 214-29.

524 25. Lafarga, V., et al., *p38 Mitogen-activated protein kinase- and HuR-dependent*
525 *stabilization of p21(Cip1) mRNA mediates the G(1)/S checkpoint.* Mol Cell Biol, 2009.
526 **29**(16): p. 4341-51.

527 26. Denkert, C., et al., *Overexpression of the embryonic-lethal abnormal vision-like protein*
528 *HuR in ovarian carcinoma is a prognostic factor and is associated with increased*
529 *cyclooxygenase 2 expression.* Cancer Res, 2004. **64**(1): p. 189-95.

530 27. Denkert, C., et al., *Expression of the ELAV-like protein HuR is associated with higher*
531 *tumor grade and increased cyclooxygenase-2 expression in human breast carcinoma.*
532 Clin Cancer Res, 2004. **10**(16): p. 5580-6.

533 28. Miyata, Y., et al., *High expression of HuR in cytoplasm, but not nuclei, is associated with*
534 *malignant aggressiveness and prognosis in bladder cancer.* PLoS One, 2013. **8**(3): p.
535 e59095.

536 29. Mrena, J., et al., *Cyclooxygenase-2 is an independent prognostic factor in gastric cancer*
537 *and its expression is regulated by the messenger RNA stability factor HuR.* Clin Cancer
538 Res, 2005. **11**(20): p. 7362-8.

539 30. Lebedeva, S., et al., *Transcriptome-wide analysis of regulatory interactions of the RNA-*
540 *binding protein HuR.* Mol Cell, 2011. **43**(3): p. 340-52.

541 31. Akaike, Y., et al., *HuR regulates alternative splicing of the TRA2beta gene in human*
542 *colon cancer cells under oxidative stress.* Mol Cell Biol, 2014. **34**(15): p. 2857-73.

543 32. Davis, C.A., et al., *The Encyclopedia of DNA elements (ENCODE): data portal update.*
544 Nucleic Acids Res, 2018. **46**(D1): p. D794-D801.

545 33. EncodeProjectConsortium, *An integrated encyclopedia of DNA elements in the human*
546 *genome.* Nature, 2012. **489**(7414): p. 57-74.

547 34. Jakstaite, A., et al., *HuR mediated post-transcriptional regulation as a new potential*
548 *adjuvant therapeutic target in chemotherapy for pancreatic cancer.* World J
549 Gastroenterol, 2015. **21**(46): p. 13004-19.

550 35. Tran, H., F. Maurer, and Y. Nagamine, *Stabilization of urokinase and urokinase receptor*
551 *mRNAs by HuR is linked to its cytoplasmic accumulation induced by activated mitogen-*

activated protein kinase-activated protein kinase 2. Mol Cell Biol, 2003. **23**(20): p. 7177-88.

36. Wang, W., et al., *HuR regulates p21 mRNA stabilization by UV light.* Mol Cell Biol, 2000. **20**(3): p. 760-9.

37. Dolado, I., et al., *p38alpha MAP kinase as a sensor of reactive oxygen species in tumorigenesis.* Cancer Cell, 2007. **11**(2): p. 191-205.

38. Emerling, B.M., et al., *Mitochondrial reactive oxygen species activation of p38 mitogen-activated protein kinase is required for hypoxia signaling.* Mol Cell Biol, 2005. **25**(12): p. 4853-62.

39. Huang, S., et al., *Urokinase plasminogen activator/urokinase-specific surface receptor expression and matrix invasion by breast cancer cells requires constitutive p38alpha mitogen-activated protein kinase activity.* J Biol Chem, 2000. **275**(16): p. 12266-72.

40. Carduner, L., et al., *Cell cycle arrest or survival signaling through alphav integrins, activation of PKC and ERK1/2 lead to anoikis resistance of ovarian cancer spheroids.* Exp Cell Res, 2014. **320**(2): p. 329-42.

41. Liao, W.L., et al., *The RNA-binding protein HuR stabilizes cytosolic phospholipase A2α mRNA under interleukin-1β treatment in non-small cell lung cancer A549 Cells.* J Biol Chem, 2011. **286**(41): p. 35499-508.

42. Ishimaru, D., et al., *Regulation of Bcl-2 expression by HuR in HL60 leukemia cells and A431 carcinoma cells.* Mol Cancer Res, 2009. **7**(8): p. 1354-66.

43. Levy, N.S., et al., *Hypoxic stabilization of vascular endothelial growth factor mRNA by the RNA-binding protein HuR.* J Biol Chem, 1998. **273**(11): p. 6417-23.

44. Prislei, S., et al., *MiR-200c and HuR in ovarian cancer.* BMC Cancer, 2013. **13**: p. 72.

45. Slone, S., et al., *Activation of HuR downstream of p38 MAPK promotes cardiomyocyte hypertrophy.* Cell Signal, 2016. **28**(11): p. 1735-41.

46. Doller, A., et al., *Tandem phosphorylation of serines 221 and 318 by protein kinase Cdelta coordinates mRNA binding and nucleocytoplasmic shuttling of HuR.* Mol Cell Biol, 2010. **30**(6): p. 1397-410.

47. Grammatikakis, I., K. Abdelmohsen, and M. Gorospe, *Posttranslational control of HuR function.* Wiley Interdiscip Rev RNA, 2017. **8**(1).

48. Fazzone, H., A. Wangner, and L.B. Clerch, *Rat lung contains a developmentally regulated manganese superoxide dismutase mRNA-binding protein.* J Clin Invest, 1993. **92**(3): p. 1278-81.

49. Chung, D.J., A.E. Wright, and L.B. Clerch, *The 3' untranslated region of manganese superoxide dismutase RNA contains a translational enhancer element.* Biochemistry, 1998. **37**(46): p. 16298-306.

50. Chaudhuri, L., et al., *Preferential selection of MnSOD transcripts in proliferating normal and cancer cells.* Oncogene, 2012. **31**(10): p. 1207-16.

51. Church, S.L., *Manganese superoxide dismutase: nucleotide and deduced amino acid sequence of a cDNA encoding a new human transcript.* Biochim Biophys Acta, 1990. **1087**(2): p. 250-2.

52. Sugiura, A., et al., *Newly born peroxisomes are a hybrid of mitochondrial and ER-derived pre-peroxisomes.* Nature, 2017. **542**(7640): p. 251-254.

53. Tenenbaum, S.A., et al., *Ribonomics: identifying mRNA subsets in mRNP complexes using antibodies to RNA-binding proteins and genomic arrays.* Methods, 2002. **26**(2): p. 191-8.

54. Dang Do, A.N., et al., *eIF2alpha kinases GCN2 and PERK modulate transcription and translation of distinct sets of mRNAs in mouse liver.* Physiol Genomics, 2009. **38**(3): p. 328-41.